Sparsity constraints and dedicated acquisition protocols for improved Digital Subtraction Rotational Angiography

Hélène Langet, C. Riddell, Y. Trousset, Elisabeth Lahalle, Arthur Tenenhaus, Gilles Fleury, Nikolaos Paragios

Sparsity constraints and dedicated acquisition protocols for improved Digital Subtraction Rotational Angiography

Hélène Langet[1,2,3], Cyril Riddell[1], Yves Trousset[1], Elisabeth Lahalle[3], Arthur Tenenhaus[3], Gilles Fleury[3], and Nikos Paragios[2]

***Abstract*—Digital Subtraction Rotational Angiography (DSRA) allows reconstruction of three-dimensional vascular structures from two spins: the contrast is acquired after injecting vessels with a contrast medium, whereas the mask is acquired in the absence of injection. The vessels are then detected by subtraction of the mask from the contrast. Standard DSRA protocol samples the same set of equiangular-spaced positions for both spins. Due to technical limitations of C-arm systems, streak artifacts degrade the quality of all three reconstructed volumes.**

Recent developments of compressed sensing have demonstrated that it is possible to recover a signal that is sparse in some basis under limited sampling conditions. In this paper, we propose to improve the reconstruction quality of non-sparse volumes when there exists a sparse combination of these volumes. To this purpose, we develop an extension of iterative filtered backprojection that jointly reconstructs the mask and contrast volumes via ℓ_1-minimization of sparse priors. A dedicated protocol based upon interleaving both spins is shown to further benefit from the sparsity assumptions, while using the same total number of measurements.

Our approach is evaluated in parallel geometry on simulated phantom data.

***Index Terms*—Digital Subtraction Angiography, Rotational angiography, Compressed sensing, ℓ_1-minimization, Iterative reconstruction**

I. Introduction

In interventional radiology, one of the main purposes is the visualization of vascular structures. Since vessels inherit contrast comparable to the one of encompassing tissues, they are imaged by injecting a radio-opaque contrast medium into the blood.

In rotational angiography, a tomographic acquisition (spin) of two-dimensional (2D) X-Ray projection views is used to reconstruct a three-dimensional (3D) model of the injected vessels in their environment. However, it might be difficult to separate the vascular structures from surrounding bones or dense devices such as coils. This can be circumvented by performing two acquisitions in a single protocol, similarly to 2D Digital Subtracted Angiography (DSA) [1]. The first acquisition, called mask, is performed without injection, while the second acquisition, called contrast, is performed after vessel opacification. All structures but the vessels are removed by digital subtraction of the mask volume from the contrast volume. One can thus visualize either the vessels alone (subtracted volume), or the vessels and their context (contrast volume) or the context alone (mask volume of bones, tissues and devices).

DSRA is more challenging than DSA, because the injection must be such that all vessels located inside the field of view are fully opacified from the beginning to the end of the contrast spin. The contrast medium is however rapidly flushed in the blood flow. To minimize contrast use, the rotation of the C-arm has to be as fast as possible, while its acquisition frame rate is limited, which significantly restricts the angular sampling. Subsampling has little incidence on visualization of highly contrasted structures, but it generates streak artifacts that hide weakly contrasted structures such as soft tissues. To reconstruct a satisfying subtracted volume, the mask and contrast spins are traditionnally acquired with identical parameters, which allows the straightforward removal of redundant background structures and their associated streaks.

Standard reconstruction of the mask and contrast volumes is obtained independently. Each volume suffers from the same undersampling artifacts and the same noise level. They cannot be combined a posteriori to either reduce noise or artifacts because vessel streaks would then propagate into the mask volume.

In the following, we propose to use recent compressed sensing results to jointly reconstruct the mask and contrast volumes. Based on the assumption that vessels are sparse, we show how improved image quality can be obtained for the non-sparse background structures as well. Through a temporal interpretation of the subtraction problem, we define a coupling between the mask and contrast volumes that allows for their joint reconstruction via imposing sparse priors. We extend the iterative filtered backprojection so that vessel sparsity can be applied and promote redundance of the non-opacified structures captured in both spins. We show that adopting interleaved spins rather than identical spins allows for increasing the angular sampling of the mask and contrast volumes. Two sparsity constraints and two acquisition protocols are combined and evaluated in a numerical simulation phantom study. Potential applications of this work are finally discussed.

II. Method

Let $f = \begin{pmatrix} f_C \\ f_M \end{pmatrix}$ be the vector containing the contrast volume ($f_C \in \mathbb{R}^J$) and the mask volume ($f_M \in \mathbb{R}^J$),

The authors are with [1]GE Healthcare – 78530 Buc – France, [2]Ecole Centrale Paris – 92290 Châtenay-Malabry – France, and [3]Supélec – 91192 Gif-sur-Yvette – France.
E-mail: helene.langet@ge.com.

where J is the number of voxels. Let $p = \begin{pmatrix} p_C \\ p_M \end{pmatrix}$ be the vector containing the injected projections ($p_C \in \mathbb{R}^I$) and the mask projections ($p_M \in \mathbb{R}^I$), where I is the total number of measurements. Let $R = \mathrm{diag}\{R_C, R_M\}$ with R_C, $R_M \in \mathbb{R}^{I \times J}$ be the block-diagonal matrix describing the trajectory of the contrast and mask spins respectively. The reconstruction problem consists in recovering f given that $p = Rf$.

A. Least-squares approach

The reconstruction used in practice consists in a discretization of the analytical inverse of the system, i.e. backprojection of the filtered projections: $f = R^T Dp$, where D refers to the ramp filter. This method is known as filtered backprojection (FBP).

There exists an iterative version of FBP (iFBP), which comes round to use the euclidian norm as measure of the distance between p and the filtered projections of f:

$$\left\{ \begin{array}{rcl} f^* & = & \underset{f}{\mathrm{argmin}} Q(f) \\ Q(f) & = & \frac{1}{2} \| D^{1/2} \left(Rf - p \right) \|_2^2 \end{array} \right. \quad (1)$$

iFBP scheme is a standard gradient descent with step $\tau > 0$:

$$\left\{ \begin{array}{rcl} f^{(0)} & = & 0 \\ f^{(n+1)} & = & f^{(n)} - \tau \nabla Q(f^{(n)}) \end{array} \right.$$

FBP and iFBP provide valid solutions if the system is well-determined. When the system is underdetermined (i.e. $I << J$), typically when the number of projections is low, these methods set to zero the Fourier components that are unobservable given the measures, which is not justified from a physical point of view, and results in a volume that is deteriorated by streak artifacts.

In a general way, if $\tilde{f}$ is the solution of the fully sampled problem, it can be expressed as:

$$\tilde{f} = f^* + f^\perp \text{ where } \left\{ \begin{array}{l} f^* \text{ is the iFBP solution} \\ f^\perp \in Ker(R) \end{array} \right.$$

To reduce the magnitude of $f^\perp$, which is the error image made of complementary streak artifacts, it is necessary to constrain $\tilde{f}$ by introducing additional regularization terms to the quadratic functional.

B. Compressed sensing approach

In [2] [3] notably, it is demonstrated that it is possible to recover a signal from a small number of measurements if it is sparse in some basis, that is, if most of the signal energy is concentrated in a few coefficients only. In practice, minimization of the ℓ_1-norm promotes sparsity [4] and is applied for generating sparse approximations of undersampled signals.

We define a functional J as the sum of a quadratic data fidelity term Q and a sparsity penalty φ, i.e $J(f) = Q(f) + \varphi(f)$. The function Q is convex and differentiable, whereas φ is convex and non-differentiable due to the singularity of the ℓ_1-norm. This excludes the use of conventional smooth optimization techniques.

Combettes and Pesquet [5] have shown that it is possible to reach convergence with a simple implementation that consists in an explicit gradient step for minimizing Q (in our case iFBP) and an implicit step applying the constraint φ:

$$\left\{ \begin{array}{rcl} f^{(n+1/2)} & = & f^{(n)} - \tau \nabla Q(f^{(n)}) \\ f^{(n+1)} & = & \mathrm{prox}_{\tau,\varphi} \left(f^{(n+1/2)} \right) \end{array} \right. \quad (2)$$

where the penalization is applied via its proximity operator defined as:

$$\forall x \in \mathbb{R}^J, \quad \mathrm{prox}_{\gamma,\varphi} : x \to \underset{y \in \mathbb{R}^J}{\mathrm{argmin}} \left[\varphi(y) + \frac{1}{2\gamma} \|x - y\|_2^2 \right]$$

where $\gamma > 0$ and is set equal to the gradient step τ in (2).

Several accelerated implementations of (2) have been proposed. In practice, we used the Fast Iterative Shrinkage Thresholding Algorithm (FISTA) [6].

C. Temporal interpretation

DSRA can be viewed as a temporal acquisition with two time points t_O and t_M, such that $f_C = f(t_C)$ and $f_M = f(t_M)$. It is possible to define an invertible temporal transform H_t such that at least one of the components of $H_t f$ is sparse.

Here H_t is the operator associated with the one-dimensional (1D) Haar wavelet transform:

$$H_t = \begin{bmatrix} 1 & 1 \\ 1 & -1 \end{bmatrix}$$

Define w by $w = \begin{pmatrix} w_1 \\ w_2 \end{pmatrix} = H_t f = \begin{pmatrix} f_C + f_M \\ f_C - f_M \end{pmatrix}$. The vector w_2 corresponds to the subtracted volume which contains vascular structures only, and as such, is intrinsically sparse. The use of H_t thus allows for isolating the sparse structures induced by contrast injection.

1) Soft-thresholded (ST) reconstruction: ℓ_1 penalization through $\|w_2\|_1$ has already been successfully applied to the dynamic reconstruction of naturally sparse volumes such as the coronary arteries [7]. In our case of DSRA, we expect that the sparsity constraint on w_2 will promote in f the redundance of the non-opacified structures captured in both spins. We thus minimize the following functional:

$$J_{ST}(f) = Q(f) + \lambda \|w_2\|_1 \quad (3)$$

where λ is the regularization parameter that allows for controlling the strength of the ℓ_1-penalization. In this case, the proximal operator corresponds to soft-thresholding: $\mathrm{S}_{\lambda\tau}(w_2)$ of threshold $\lambda\tau$ where τ is the step defined in (2). By minimizing J_{ST}, the maximal sampling that can be achieved for w_1 cannot exceed the addition of the mask and the contrast sampling.

2) Total Variation (TV) reconstruction: The addition of the mask and the contrast sampling may still result in an undersampled problem. Since w_1 is not naturally sparse, an efficient method consists in promoting sparsity of $TV(w_1) = \|\nabla w_1\|_1$ [2]. The corresponding solution is a piece-wise constant approximation of w_1. Furthermore, the subtracted volume often contains not only vessels, but also perfused structures such as parenchyma that can be approximated by piecewise constant

distributions. Thus, we propose to minimize $TV(w_2)$ as well. The corresponding functional is:

$$J_{TV}(f) = Q(f) + \lambda_1 \|\nabla w_1\|_1 + \lambda_2 \|\nabla w_2\|_1 \qquad (4)$$

To minimize (4), the digital TV filter [8] is used as proximal operator of $\|\nabla \cdot\|_1$. This filter is applied to w_1 with strength $\lambda_1\tau$ and to w_2 with strength $\lambda_2\tau$. In order to minimize bias in the estimation of w_1, we set $\lambda_1 << \lambda_2$.

3) Data acquisition: We consider N equiangular-spaced views of the contrast and mask volumes with two protocols:

- *Homogeneous* protocol: this is the standard DSRA acquisition where the trajectories of each spin samples the same set of angular positions:

$$A_C = A_M = \{\alpha_n = \frac{n}{N-1}\cdot\alpha_{range} \quad | \quad n = 0 \cdots N-1\}$$

- *Heterogeneous* protocol: alternatively each spin samples two sets of interleaved angular positions defined by:

$$\begin{cases} A_M &= \{\alpha_n = \frac{n}{N-1} \cdot \alpha_{range} \quad | \quad n = 0 \cdots N-1\} \\ A_C &= \{\alpha_n = \frac{n+\delta}{N-1} \cdot \alpha_{range} \quad | \quad n = 0 \cdots N-1\} \end{cases}$$

where $\delta =]0, 1[$ is the angular shift.

Standard DSRA uses redundance of the non-opacified structures in the mask and contrast views to obtain the vessels without background streaks, which is only possible using the homogeneous protocol.

Introduction of sparsity assumptions based on the minimization of J_{ST} or J_{TV} will also remove background streaks in the subtracted volume, whatever the acquisition protocol. However, when interleaving the contrast and mask spins, the angular sampling of the non-opacified structures is increased. In particular, with $\delta = 0.5$, background structures are sampled with $2N$ equiangular-spaced views, whereas the vessels are sampled with N equiangular-spaced views.

III. Results

Minimization of J_{ST} and J_{TV} was evaluated for each acquisition protocol in parallel geometry on a 2D numerical simulation phantom.

A. Simulations

In order to simulate a realistic anatomy, we used a true abdominal CT cross-section (Fig. 1(a) and Fig. 1(b)) as mask image. We obtained the contrast image by adding to the mask four intense disks (Fig. 1(c)) that represent strongly opacified arteries. Intensities are given in Hounsfield Unit (HU). The value of simulated injected vessels is about 3000 HU, while values of soft tissues are those of the original CT slice, around 0 HU. Acquisitions were simulated with 150 views over $180°$. The angular shift $\delta = 0.5$ was used for the heterogeneous protocol.

FISTA for iFBP was run for 100 iterations with step $\tau = 0.1$. We set $\lambda = 10$ in J_{ST} and $\lambda_2 = 10$ in J_{TV}. λ_1 in J_{TV} was set to 1, i.e. one tenth of the penalization strength applied on w_2.

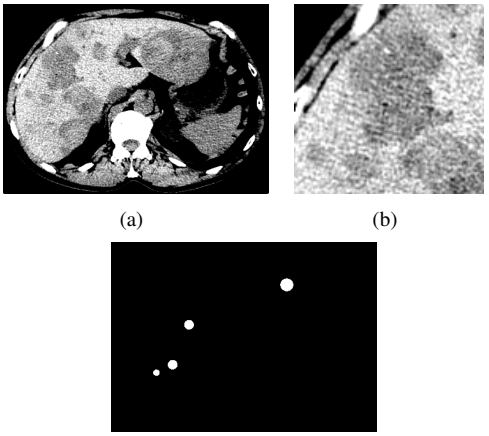

(a) (b)

(c)

Fig. 1. Numerical simulation phantom. (a) Mask image; (b) Details of (a); (c) Simulated vessels.

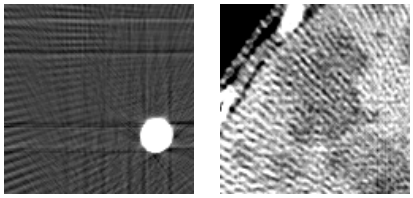

(a) (b)

Fig. 2. FBP reconstruction from 150 views. (a) Details of the vessels; (b) Details of the mask image. WC = 60 HU and WW = 75 HU.

B. Evaluation

Images are visualized with a windowing of window center (WC) 60 HU and window width (WW) 75 HU.

FBP reconstruction from 150 views, which is the current level of image quality in clinical routine, is displayed in Fig. 2. Fig. 2(a) shows details of the vessel streaks that actually degrade the entire field of view, while Fig. 2(b) shows details of the background streaks.

Both J_{ST} and J_{TV} perfectly restored the vessels, since they verify the sparsity constraints, by setting to zero all non-vessel pixels. Consequently mask and contrast reconstructions shared the same background. Artifact level in the background depended on both acquisition protocol and sparsity constraint. This level was quantified by computing over the J_b pixels of the background structures the root mean square deviation (RMSD) between the reconstruction and the reference $d = \sqrt{\frac{1}{J_b}\sum_{j=1}^{J_b}\left(f_j - \tilde{f}_j\right)^2}$.

Fig. 3(a) and Fig. 3(b) show that the minimization of J_{ST} from homogeneous spins did not improve the quality of the background over FBP. RMSD values are equivalent in these two cases: $d = 18$ HU. On the opposite, Fig. 3(c) and Fig. 3(d) show that the heterogeneous protocol allowed for reducing streak artifacts and benefited from a sampling of twice as many views. The RMSD d was reduced to 11 HU.

Fig. 4 shows that the use of TV resulted in less streaks in the homogeneous protocol (Fig. 4(a)) as well as in the heterogeneous protocol (Fig. 4(c)). The RMSD was $d = 13$ HU in the homogeneous case and was reduced to $d = 11$ HU in the heterogeneous case. Figure details (Fig. 4(b) and Fig.

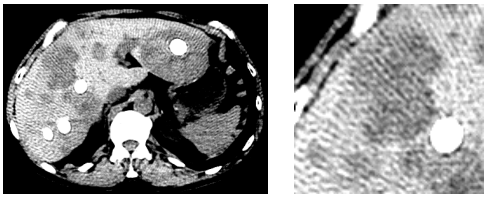

(a) (b)

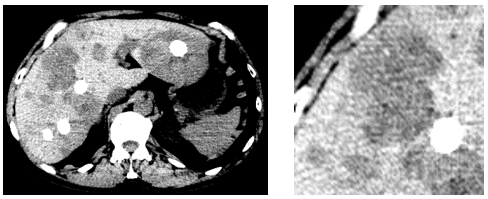

(c) (d)

Fig. 3. Reconstruction by minimization of J_{ST} from 150 views. WC $=$ 60 HU and WW $=$ 75 HU. (a) Reconstruction of the contrast from homogeneous spins; (b) Details of (a); (c) Reconstruction of the contrast from heterogeneous spins; (d) Details of (c).

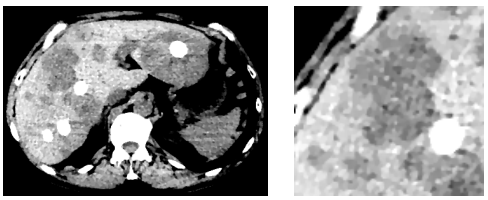

(a) (b)

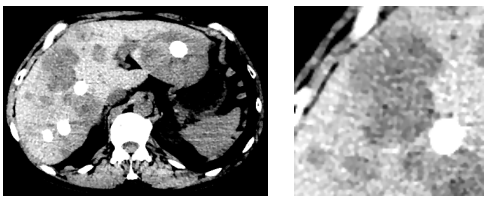

(c) (d)

Fig. 4. Reconstruction by minimization of J_{TV} from 150 views. WC $=$ 60 HU and WW $=$ 75 HU. (a) Reconstruction of the contrast from homogeneous spins; (b) Details of (a); (c) Reconstruction of the contrast from heterogeneous spins; (d) Details of (c).

4(d)) also highlight that the piecewise-constant approximation implied by TV affected the overall texture of the background.

IV. Discussion

Soft-thresholded reconstruction did not improve the image quality when spins are homogeneous, even though the simulated vessels verified the sparsity hypothesis. In this latter case, the use of an heterogeneous protocol was required to raise image quality without introducing a bias. However, natural sparsity does not generalize to contrast distributions that may be found in perfused tissues. Reconstruction penalized by TV gave decreased artifact levels, whatever the acquisition protocol, at the expense of a change in the overall texture of the background that may not be clinically acceptable. Still, these results suggest dose reduction strategies. On the one hand, it should be possible to reduce the noise (simultaneously to the reduction of the streaks) and raise image quality, at constant dose level. On the other hand, one could reduce the dose by half without deteriorating image quality.

Confirmation of the applicability of the proposed algorithms in cone-beam geometry and on clinical data is on-going.

Compressed sensing penalties were selected in this work according to the acquisition pattern at hand. An alternative sparsity penalty has been proposed in PICCS [9], which relies on a prior image. If the mask image is taken as the prior image, the redundant background structures will be set to the mask and will not be improved further. The sum of the mask and contrast volumes cannot be taken as prior, since it is degraded by vessel streaks. The PICCS approach rather suggests an unbalanced acquisition protocol where many views would be dedicated to sampling the mask, while the contrast volume would be estimated from very few contrast projections and a prior image equal to the mask.

V. Conclusion

Extension of iterative filtered backprojection with ℓ_1-minimization has been presented for X-ray Digital Subtraction Rotational Angiography. Evaluation on a simulated phantom in parallel geometry showed that sparsity constraints on vessels allowed to generate streak-free vessel images. More interestingly, the non-sparse non-injected structures were estimated from both mask and contrast acquisition, thus benefiting from an increased angular sampling that reduced the streak level. Overall image quality depended on the selected penalties and acquisition protocols. A simple angular shift between the mask and the contrast acquisition resulted in artifact reduction, whatever the sparsity constraint. This suggests strategies for either reducing the dose or improving the image quality of current clinical X-ray DSRA exams.

References

[1] W. R. Brody, "Digital subtraction angiography," *IEEE Transactions on Nuclear Science*, vol. 29, no. 3, pp. 1176–1180, 1982.

[2] E. Candès, J. Romberg, and T. Tao, "Robust Uncertainty Principles: Exact Signal Reconstruction from Highly Incomplete Frequency Information," *IEEE Transactions on Information Theory*, vol. 52, no. 2, pp. 489–509, 2006.

[3] Starck, Elad, and Donoho, "Image decomposition via the combination of sparse representations and a variational approach," *IEEE Transactions on Image Processing*, vol. 14, pp. 1570–1582, 2004.

[4] D. Donoho, "For most large underdetermined systems of linear equations, the minimal ℓ_1 solution is also the sparsest solution," *Comm. Pure Appl. Math.*, vol. 59, pp. 797–829, Jun. 2006.

[5] P. L. Combettes and J.-C. Pesquet, "Split convex minimization algorithm for signal recovery," in *Accoustics, Speech and Signal Processing, 2009. ICASSP 2009. IEEE International Conference on*, Apr. 2009, pp. 685–688.

[6] A. Beck and M. Teboulle, "A fast iterative shrinkage-thresholding algorithm for linear inverse problems," *SIAM Journal on Imaging Sciences*, vol. 2, pp. 183–202, March 2009.

[7] E. Hansis, D. Schäfer, O. Dössel, and M. Grass, "Evaluation of iterative sparse object reconstruction from few projections for 3-D rotational coronary angiography," *IEEE Transactions on Medical Imaging*, vol. 27, no. 11, pp. 1548–1555, Nov. 2008.

[8] T. F. Chan, S. Osher, and J. Shen, "The Digital TV Filter and Nonlinear Denoising," *IEEE Transactions on Image Processing*, vol. 10, no. 2, pp. 231–241, Feb. 2001.

[9] G. H. Chen, Tang, and Leng, "Prior image constrained compressed sensing (PICCS)," *Medical Physics*, vol. 35, no. 2, pp. 660–663, Feb. 2008.